A Flexible and Reconfigurable Si_3N_4 ROADM-enabled 5G mmWave IFoF Fiber Wireless Fronthaul with 60 GHz beamsteering capabilities

A. Tsakyridis(1), E. Ruggeri(1), G. Kalfas(1), R.M. Oldenbeuving(2), P.W.L. van Dijk(2), C. Roeloffzen(2), Y. Leiba(3), A. Miliou(1), N. Pleros(1), and C. Vagionas(1)
[1] Department of Informatics, Center for Interdisciplinary Research & Innovation, Aristotle University of Thessaloniki, Thessaloniki, Greece
[2] LIONIX International B.V., Enschede, The Netherlands
[3]Siklu Communication Ltd., Petach Tikva, 49517, Israel
atsakyrid@csd.auth.gr

Abstract *A bandwidth-reconfigurable mmWave Fiber Wireless fronthaul bus topology of four 1 Gb/s 16-QAM streams transmitted through two cascaded low-loss Si_3N_4-ROADM stages and a 60 GHz Phased Array Antenna with 90° steering is experimentally demonstrated the first time for 5G C-RANs.*

Introduction

With the advent of 5G, emerging Use Cases of enhanced Mobile Broadband Services (eMBB) or Fixed Wireless Access (FWA)[1] are driving an insatiable need for broadband connectivity with up to 1Gb/s user rate, low-latency, high mobility, coverage and reliability etc.[1]. The drastic surge of mobile traffic by millimetre Wave (mmWave) in the Radio Access Network (RAN) is expected to overload the optical fronthaul links, promoting more spectrally efficient analog Radio over Fiber (RoF) transport schemes[2]. Profound Fiber Wireless (FiWi) A-RoF/mmWave links already achieved several radio-channels with user rates beyond 1 Gb/s and capacities larger than 10 Gb/s[3]-[6], penetrating field-deployed legacy PONs[7] or rail networks[8] and satisfying the respective 5G KPIs for data rates and mobility. However, these demonstrations have so far mostly relied on single static Point-to-Point (PtP) backhaul links between fixed horn antennas with optimized power-budget and linear-regime and only very recently were mmWave Phased Array Antennas (PAAs) interfaced with A-RoF scheme to enable single steerable PtP FiWi beams in the 28 GHz[9][10] or 60 GHz band[11][12].

However, the time-varying features of mobile traffic require an adaptive and reconfigurable network with flexible bandwidth allocation based on user needs[13]-[15] e.g. from a more evenly distributed FWA traffic to a peak, temporarily localized eMBB traffic at hotspots or nomadic traffic of high mobility in trains[8]. Centralized RAN architectures operated over Point-to-Multi-Point (PtMP) physical topologies are expected to bring the benefits of statistical multiplexing of hardware resources by deploying low-cost, small optical switches or Reconfigurable Optical Add/Drop Multiplexers (ROADMs)[15]-[18]. In particular, Silicon Photonics (SiPho) featuring CMOS compatibility and mature integration can facilitate such miniaturized, high-bandwidth and low-cost devices, being lately deployed in D-RoF C-RANs of 10 Gb/s CPRI links by Ericsson [17]-[19], while low optical losses are of critical importance for the challenging power budgets of analog fronthauls[12]. Consequently, analog FiWi reconfiguration has so far been limited only to SiPho wavelength selective switches with >10 dB losses[20], costly-bulky Wavelength Selective optical Switches[21],[22], as well as static horn-to-horn links[21]-[23] or even wired RoF setups only [20], not managing to meet their strict budget requirements and validate their suitability for

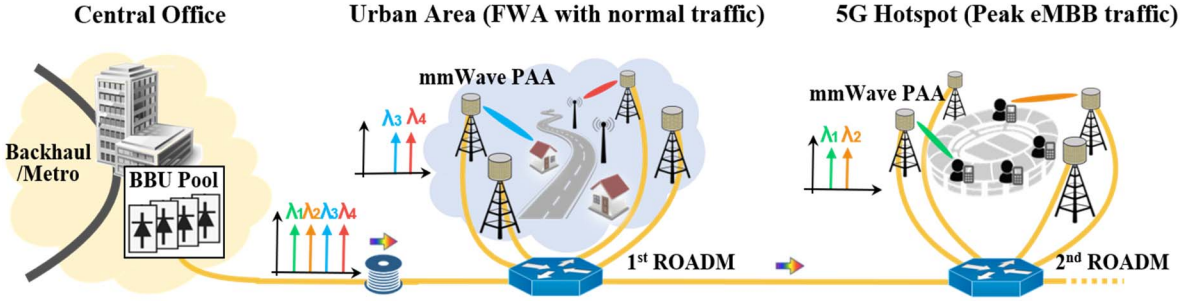

Fig. 1: Reconfigurable optical transport network concept, fronthauling mmWave PAAs to serve dense and hotspot areas.

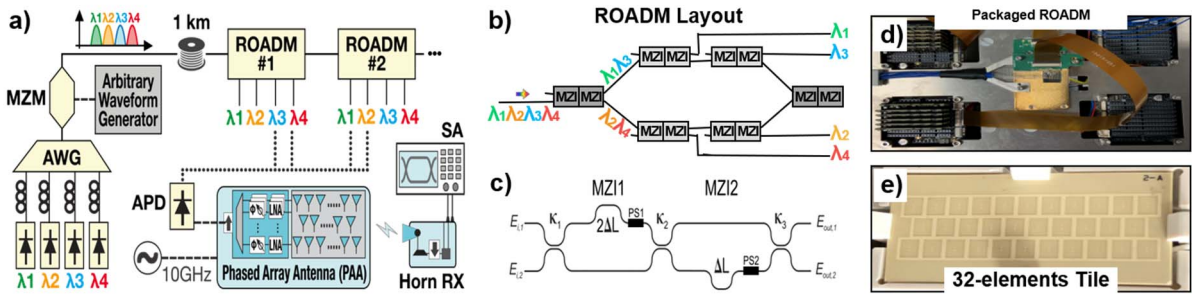

Fig. 2: a) Experimental Setup, b) ROADM Layout, c) MZI-building block, d) Packaged ROADM, e) 32- antenna element Tile.

flexible reconfigurable C-RANs.

In this paper, we experimentally demonstrate for the first time a two-stage bandwidth-reconfigurable mmWave FiWi fronthaul bus topology for flexible and efficient C-RANs. The proposed architecture includes four 1 Gb/s FiWi IFoF/mmWave channels configured among two cascaded stages of four port Si_3N_4 ROADMs with 100 GHz lattice filter design and only 5 dB fiber-to-fiber loss. Supporting in total eight V-band PAA terminals with 32-radiating elements and 90° beamsteering per channel, bandwidth reconfigurability is demonstrated by selectively dropping each optical stream to the first or the second ROADM-stage of the fronthaul bus, allowing for on-demand re-allocation of network resources. Carrying 250 Mbd 16-QAM to meet the 1 Gb/s KPI maximum User Rate requirement and featuring EVM values that meet the 3GPP EVM limits, the proposed FiWi IFoF/mmWave fronthaul bus paves the way towards both spectrally efficient and flexible, reconfigurable mmWave C-RANs for 5G and beyond.

Devices and Experimental Setup

The experimental setup of the two-stage FiWi IFoF transmission is shown in Fig. 2 a). Initially, a 4λ-WDM IFoF stream is generated by multiplexing four λ_1-λ_4 Continuous Wavelengths (CWs) spaced by 100 GHz at 1545.6 nm, 1546.4 nm, 1547.2 nm and 1548 nm. The CWs are modulated by a $LiNbO_3$ Mach Zehnder Interferometer (MZI) modulator, biased at the quadrature point and driven by an Arbitrary Waveform Generator using a 250 Mbd 16-QAM waveform on an 5 GHz IF to generate four 1 Gb/s Double Side-Band (DSB) IFoF streams of around 4.8 dB power per wavelength. The 4λ WDM stream is launched at 1 km-long SMF spool before passing the two cascaded ROADM stages spaced by 100 m SMF in bus topology.

Aiming to reconfigurably interconnect the channels of the network grid with negligible distortion of IFoF signals, each ROADM channel can filter an optical carrier and the two side bands with flat top response and negligible power variation across the channel bandwidth. The layout of the ROADM layout was designed as a lattice, cascaded MZI-interleaver in Add/Drop configuration shown in Fig. 2 b), exhibiting 100 GHz spacing, 32.5 GHz flat-top pass-band and less than <0.02 dB power variation between the upper/lower sideband [16]. Integrated on an ultra-low loss Si_3N_4/SiO_2 TriPleX platform [24], the ROADM exhibits only 5 dB fiber-to-fiber losses., while any non-ideal filter transfer function can be compesnated by the tunable optical couplers at the MZIs shown in Fig. 2 c). The ROADM was fully packaged on a TEC-PCB with wire-bonds and fiber array as bench-top solution, as shown in Fig. 2 d).

The four Drop ports at the output of each ROADM, featuring an average optical output power of -0.4 dBm and -5.4 dBm after the 1st and 2nd stage respectively, were reconfigurably connected to the antenna site, where each stream was O/E converted by a 10 GHz InGaAs Avalanche Photodiode (APD) and fed as input to the PAA for wireless transmission. The PAA featured an integrated upconversion stage, fed by external 10 GHz Oscillator, comprising 32 channels of RF phase shifters and Low Noise Amplifiers (LNAs). All channels are connected to radiating dipoles of 6 dBi gain, integrated on a low-temperature ceramics-substrate Tile PCB for homogeneity, rigidity and consistent dielectric constant over temperature, assembled at the frontpanel, as shown in Fig. 2 e). The PAA is controlled by a Control PCB board for tuning each phase shifter per element for beamsteering purposes. When all elements are activated, the PAA forms a 10^0-wide beam, steered across 90^0, powered by 5.3 V and 1.6 A. Finally, after 1m V-band link, the signal is received by a portable Rx horn with 22.5 dBi gain, dedicated down-conversion stage and I/Q demodulator, that is connected to a Signal Analyzer (SA) for monitoring purposes, building four reconfigurable FiWi IFoF/mmWave links, dropped at the first or at the second stage.

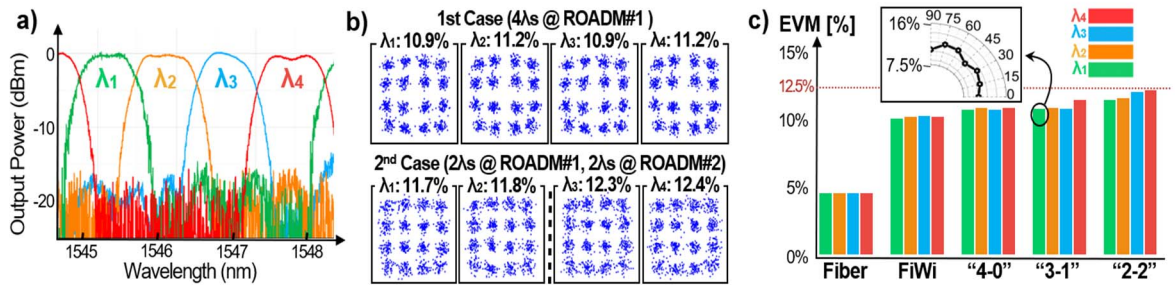

Fig. 3: a) Transfer function of the ROADM, b) Constellation diagrams of the 1st case (4λs dropped @ROADM1) and the 2nd case (2λs dropped @ROADM1 and 2λs dropped @ROADM2, c) EVM comparison of the investigated scenarios.

Experimental Results

Initially, the ROADM was statically characterized by inserting ASE noise at the input port and evaluating the spectrum at each drop port using an Optical Spectrum Analyzer. The channel spectra superimposed using different coloring are shown in Fig. 3 a), featuring a flat-top response across at least 0.25 nm and 3 dB bandwidth of 0.66 nm, while the crosstalk between the pass-band at the central peak compared to the stop band of neighboring channels was at least 18 dB, allowing clear demultiplexing of IFoF streams. Then, FiWi transmission through the 1st ROADM stage was performed, where all four λ_1-λ_4 250 Mbd 16-QAM streams were demultiplexed and dropped at the four ports and wirelessly transmitted by the PAA at 45^0. The received signals in Fig. 3 b) reveal clearly demodulated constellation diagrams with average 11.1% EVM.

Subsequently, the two ROADM stages were reconfigured to drop two of the four wavelength-streams at the 1st stage, namely λ_3 and λ_4, while λ_1 and λ_2 propagated to the Through port of the 1st stage and Dropped at the respective Drop ports of the 2nd stage. All four λ_1-λ_4 streams were again wirelessly transmitted by the PAA and the received constellation diagrams are shown in Fig. 3 b). As it can be seen, λ_3 and λ_4 of the 2nd stage feature slightly degraded EVM performance of 12.3% and 12.4% compared to the 11.7% and 11.8% of λ_1 and λ_2 at the 1st ROADM respectively. Also, a small degradation of λ_1 and λ_2 was observed compared to the first transmission scenario when all λ_1-λ_4 were dropped at the 1st stage, resulting in 0.6% EVM penalty, mainly attributed to a residual thermal cross-talk during ROADM reconfiguration. Nevertheless, all EVM values are within the 3GPP upper limit requirements[25], while meeting the KPIs for 1 Gb/s user rate.

Finally, aiming to investigate the scalability of the devices, we evaluated the degradation at each stage of the link by comparing five transmission scenarios: i) IFoF wired transmission only, ii) simple FiWi without interleaved ROADM, iii) FiWi with all four λs dropped at the 1st ROADM, termed as "4-0", iv) FiWi with 3 and 1 λs dropped at the 1st and 2nd stage, respectively, "3-1", and v) FiWi with 2 and 2 λs dropped at the 1st and 2nd stage, respectively, "2-2", measuring the EVM values for all channels as shown for each case with coloring per channel in Fig. 3 c). The average EVM between all channels, when these were transmitted in IFoF, simple FiWi, FiWi dropped at the 1st ROADM stage and FiWi dropped at the 2nd ROADM stage, was 4.7%, 10.5%, 11.2% and 12.4% respectively, revealing that the V-band radio is the main source of degradation, adding +5.8% average penalty between fiber-only setup (1st group) and simple FiWi (2nd group), while the pass from one ROADM stage adds only a small degradation with average penalty of 1% for all channels. Finally, the λ_1 channel after being dropped at the 1st ROADM stage was evaluated in beamsteering operation, steered with steps of 15^0 covering a sector range from -45^0 to $+45^0$ degrees, measuring the EVM values for all seven angular positions, as shown in the polar EVM plot at Fig. 3(c) inset, showing equal response across 90^0.

Conclusions

A novel four port ROADM device fabricated in a low-loss Si_3N_4 TriPlex waveguide platform is presented for 5G IFoF/mmWave fronthaul networks, enabling a reconfigurable optical bus topology of four 1Gb/s FiWi links.

Acknowledgements

The work is supported by H2020 5GPPP Phase II project 5G-PHOS (761989) and 5G STEP-FWD (722429). The authors would like to acknowledge Keysight for supporting the experiments with measurement equipment.

References

[1] Next Generation Mobile Networks Alliance, "NGMN 5G White Paper," Feb. 2019.

[2] G. Kalfas, et. al."Next Generation Fiber-Wireless Fronthaul for 5G mmWave Networks", IEEE Com.

Mag., 57 (3), 138, Mar. 2019

[3] N. Argyris, et. al. "A 5G mmWave fiber-wireless IFoF analog mobile fronthaul link with up to 24-Gb/s multiband wireless capacity," IEEE J. Lightwave Technology, vol. 37, no. 12, June 2019

[4] C. Vagionas, et.al., "A six-channel mmWave/IFoF link with 24Gb/s Capacity for 5G Fronthaul Networks," IEEE MWP, Toulouse, 2018

[5] E. Martin et.al.,"28 GHz 5G radio over fibre using UF-OFDM with optical heterodyning," MWP, Beijing 2017

[6] S. Ishimura, et. al. "1.032-Tb/s CPRI-Equivalent Rate IF-Over-Fiber Transmission Using a Parallel IM/PM Transmitter for High-Capacity Mobile Fronthaul Links", IEEE J. Lightwave Technol., vol. 36, 8, 2018

[7] K. Kanta, et. al. "Analog fiber-wireless downlink transmission of IFoF/mmWave over in-field deployed legacy PON infrastructure for 5G fronthauling," OSA J. Optical Communications and Netowrking, vol. 12, no. 10, Oct. 2020

[8] A. Kanno, et.al. "High-Speed Railway Communication System Using Linear-Cell-Based Radio-Over-Fiber Network and Its Field Trial in 90-GHz Bands," IEEE J. Lightwave Technology, vol. 38, no. 1, Jan. 2020.

[9] M. Sung, et. al. "Demonstration of IFoF-Based Mobile Fronthaul in 5G Prototype With 28-GHz Millimeter wave" IEEE J. Lightwave Technol., vol. 36, no. 2, p. 601-609, Jan. 2018

[10] M. Huang, et. al. "A Full Field-of-View Self-Steering Beamformer for 5G Mm-Wave Fiber-Wireless Mobile Fronthaul," IEEE J. Lightwave Technology, vol. 38, no. 6, pp. 1221-1229, Mar. 2020

[11] E. Ruggeri, "Multi-user V-band uplink using a massive MIMO antenna and a fiber-wireless IFoF fronthaul for 5G mmWave small-cells," IEEE J. Lightwave Technology, article in press.

[12] C. Vagionas, et. al. "Linearity Measurements on a 5G mmWave Fiber Wireless IFoF Fronthaul Link with analog RF beamforming and 120° degrees steering," IEEE Communication Letters, article in press

[13] A. Oliva, et. al. "Xhaul: toward an integrated fronthaul/backhaul architecture in 5G networks," IEEE Wireless Comm. 22 (5), 2015

[14] C. Mitdsolidou, et. al. "A 5G C-RAN Optical Fronthaul Architecture for Hotspot Areas Using OFDM-Based Analog IFoF Waveforms," Applied Sciences, vol. 9, no. 19, 4059, Sep. 2019

[15] J. Kani, et. al. "Solutions for Future Mobile Fronthaul andAccess-Network Convergence," IEEE J. Lightwave Technology, vol. 35, no. 3, 2017

[16] C. Mitsolidou, et. al. "A 5G C-RAN Architecture for Hot-Spots: OFDM based Analog IFoF PHY and MAC Layer Design," EuCNC, 2019

[17] P. Iovanna, et. al. "A Future Proof Optical Network Infrastructure for 5G Transport", J. Optical Communic. and Networking, vol. 8, no. 12, 2016.

[18] S. Nakamura, "Optical Switches Based on Silicon Photonics for ROADM Application," IEEE J. Select Topics Quantum Electronics, vol. 22, no. 6, 2016

[19] V. Sorianello, et. al. "Polarization insensitive silicon photonic ROADM with selectable communication direction for radio access networks," Optics Letters, vol. 41, no. 24, 2016

[20] C. Browning, et. al. "A Silicon Photonic Switching Platform for Flexible Converged Centralized-Radio Access Networking," in IEEE Journal of Lightwave Technology, article in press, April 2020

[21] T. Kuri, et. al. "Reconfigurable Dense Wavelength-Division-Multiplexing Millimeter-Waveband Radio-Over-Fiber Access System Technologies," IEEE J. Lightwave Technology, vol. 28, no. 16, 2010

[22] B. Schrenk, et. al. "Towards Spectrum-Programmable, Mesh-Enabled Mobile xHaul through Reconfigurable WDM Overlay in Fully-Passive Networks", ICTON, July 2015.

[23] C. Lim, et. al. "Capacity Analysis for WDM Fiber-Radio Backbones With Star-Tree and Ring Architecture Incorporating Wavelength Interleaving," IEEE J. Lightwave Technology, vol. 21, no 12, 2003

[24] C. Roeloffzen, et. al. "Low-Loss Si3N4 TriPleX Optical Waveguides: Technology and Applications Overview", IEEE J. Select Topics Quantum Electronics, vol. 24, no. 4, 2018

[25] 3GPP TS 38.104, "5G; NR; Base Station (BS) radio transmission and reception", v. 15.2.0, 2018-7.